Converting Ambient Capillary Pressure Measurements to Reservoir Stress for Improved Formation Evaluation: A Novel Approach

Mohammed Al-Hamad[1], Ahmad Al-Zoukani[1], Farhan Ali[1], Shouxiang Mark Ma[2],

[1]SLB, Schlumberger Dhahran Carbonate Research Centre, 31952 Dhahran, Saudi Arabia.
[2]Saudi Aramco, Reservoir Description & Simulation Department, 31952 Dhahran, Saudi Arabia

Abstract. Relationship between capillary pressure (Pc) and water saturation (Sw), i.e., Pc curve, is essential for reservoir characterization. Pc curve measurement via centrifugation is a routine industry core analysis practice, as it is quick and non-destructive. The test, however, is almost always performed at ambient conditions, requiring calibration to in-situ stress for subsurface applications. The objective of this study is to develop a model to convert ambient Pc data to reservoir-stress Pc curve. To achieve this, carbonate and sandstone samples with porosity ranging from 16%-20% and permeability of 24-232 mD were evaluated. Pc curves were first measured using centrifugation at ambient conditions. The samples were then cleaned and prepared for measurements at a designated stress condition (i.e., 3,000 psi) using the porous-plate method. The high-stress Pc curves, at 3,000 psi, showed a shift towards higher water saturation compared to the ambient results. Using the acquired data, a previously developed model was improved to convert ambient Pc curves to reservoir stress conditions. The modified model proved robust for both carbonate and sandstone lithologies. These findings provide a practical method to convert conventional ambient Pc curves to reservoir stress; also valuable for quality control of Pc measurements at reservoir conditions.

1 Introduction

Knowledge of the relationship between capillary pressure (Pc) and water saturation (Sw), i.e., the Pc curve, in porous media is important as it controls the distribution and flowing of reservoir fluids [1-5]. In modelling saturation height function during primary drainage, Pc can be expressed as:

$$P_C = P_o - P_w = (\rho_w - \rho_o)gh = \frac{C}{R_t}\sigma cos\theta \qquad (1)$$

Where P_w and P_o are water and oil phase pressures, σ is the oil-water interfacial tension (IFT), Θ is the contact angle, ρ_w and ρ_o are the water and oil densities, respectively, g is the acceleration due to gravity, h is the height of the fluid column above the free water level (FWL), Rt is the characteristic size of pore throats, and C is a constant depending on the shape of pore throats [6-8], for example C=1 for flat sheet pores and C=2 for circular pores [9].

Various laboratory techniques exist to determine rock Pc curves, including mercury injection capillary pressure (MICP), centrifuge, and porous plate methods [1-2]. Besides these physical experiments, digital rock physics has emerged in the last decades as a viable tool for predicting capillary pressure behavior of porous media [10-14].

From Eq 1, it is obvious that Pc depends on rock properties (C, Rt), fluid property (IFT), and property of fluid-rock interaction (θ) [15-16]. Beyond these factors, reservoir confinement stress is another parameter that affect Pc curves significantly [17]. This often leads to reduced oil relative permeability as well as oil displacement efficiency [18-19]. In addition, in tight gas sand reservoirs, petrophysical properties have been shown to shift considerably based on the specific stress and pore pressure conditions at the time of measurement [20-23].

To systematically study effects of stress, we measured Pc curves using outcrop Indiana limestone samples with consistent petrophysical properties, under both ambient and confining stress to simulate reservoir conditions. Our findings indicated that high confining stress significantly restricts water desaturation, leading to irreducible water saturations up to 10% higher than at ambient condition [12-13]. A robust correlation between low and high stressed Pc curves was established. Consequently, the primary objective of this study is to investigate the universality of the developed correlation [13] across a broader range of lithologies with diverse pore geometries.

* Corresponding author: mal-hamad@slb.com

2 Materials and Techniques

2.1 Rock Samples

Nine outcrop samples, with different lithologies (limestone, dolostone, and sandstone) were used for this study (Table 1). The helium porosity and nitrogen permeability were measured using a Coretest AP-608 machine, under minimum stress of 500 psi. The samples were divided into three sets with different permeability ranges; Set 1 with a higher permeability of about 200 mD, Set 2 an intermediate permeability of about 60 mD, and Set 3 a lower permeability of about 20 mD.

Table 1. Rock samples and their properties.

Sample	Set	Lithology	L [cm]	D [cm]	Φ [%]	K [mD]
DSI-1-11	1	Dolomite	4.582	3.799	14.43	207.1
SGB-2-4		Sandstone	4.891	3.793	19.73	214.8
IND-X-1-10		Limestone	4.865	3.799	18.03	232.4
DGU-2-1	2	Dolomite	4.954	3.807	11.51	53.2
SS-1-8		Sandstone	4.929	3.789	20.6	69.2
IND-X-1-18		Limestone	4.911	3.796	17.93	62.5
DGU1-5	3	Dolomite	4.839	3.814	10.29	19.2
PR1-5		Sandstone	4.951	3.81	17.19	24.2
IND-135-1-3		Limestone	4.322	3.812	16.44	24.0

Thin sections were also prepared (Figure 1). All images are of the same magnification.

- The dolomite samples show inter-crystalline pores. Anhedral dolomite crystals appear coalesced, which reduces porosity and permeability of the sample.
- The limestone samples are made of bioclastic grains. Intergranular pores are shown in blue, with grains being cemented with sparry calcite cement.
- Sandstone samples, with a majority of quartz grains, shows intergranular primary pores in blue. Organic matter appears in black, while cement present as calcite and iron oxide appears in brown to reddish spots. Quartz overgrowth can also be observed.

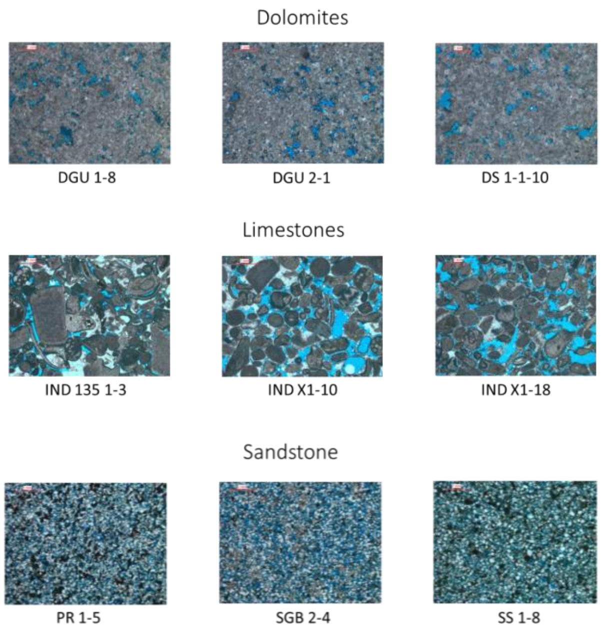

Fig. 1. Thin section images of the studied samples of dolostone, limestone, and sandstone.

2.2 Fluids

NaCl brine of 150 kppm and Soltrol-130 from Chevron Phillips were used as the two immiscible fluids for the experimentation. The fluids densities measured at 20°C are 1.110 g/cc and 0.749 g/cc, respectively. Refined oil Soltrol-130 was used to ensure that rock wettability is not one of the factors that would affect the Pc measurements, to simplify the problem, i.e., data generated from this study are for water-wet systems; applicable to primary drainage of water by oil that a zero receding contact angle may be used [24].

2.3 Experimental Procedures

The experimental procedures used in this study are listed below,

1. Prepare of core and fluid samples,
2. Measure rock properties at 500 psi,
3. Saturate the core samples with the prepared brine,
4. Use a centrifuge to conduct Pc curve tests by desaturating water with Soltrol-130, at ambient stress
5. Clean the core samples using standard Soxhlet cleaning procedures.
6. Re-measure rock properties at 500 psi and 3,000 psi,
7. Saturate the core samples with the prepared brine,
8. Use porous plate method to conduct Pc curve measurement by desaturating the brine with Soltrol-130, at a high stress.

2.4 Centrifuge Pc Tests At Ambient Stress

To conduct a Pc test by using the centrifuge method, a set of three samples in core holders separated by 120 deg is used to ensure a balanced centrifugation. For a primary drainage, the brine saturated samples are placed in the centrifuge and rotated at an RPM (revolutions per minute) increasing from low (close to zero) to the designed maximum. The centrifugal force displaces the brine with oil in the sample. The volume of produced brine at each RPM is measured to calculate the average water saturations, $S_{w,avg}$.

Pc, the pressure at the inlet face of the core, is calculated using the below equation

$$P_c = \frac{\omega^2 \Delta\rho (r_2{}^2 - r_1{}^2)}{2} \quad (2)$$

where Δρ is the density difference of the two fluids used, r_2 is the arm length from the rotor to the outer face of the core sample, r_1 is the arm length from the rotor to the inner face of the sample, and ω is the angular velocity (radians per second), which is RPM*π/30.

Using the procedures discussed in our recent publication [13], a pseudo Pc curve is generated from the raw data, by plotting Pc (Eq.2) vs $S_{w,avg}$. Water saturation at the inlet face, Sw, corresponding to Pc, needs to be inverted from $S_{w,avg}$ using methods such as Hassler-Brunner model [13]. This study isolates key variables by focusing exclusively on the standard Hassler core holder configuration, building on previous model evaluations [25].

$$S_w(P_c) = a_1 S_{wavg} + a_2 P_c \frac{dS_{wavg}}{dP_c} + E \qquad (3)$$

where a1, a2 and E are correction coefficients and often defaulted to 1, 1 and 0, respectively.

To calculate the derivative $\frac{dS_{avg}(P_{c1})}{dP_{c1}}$, a power-law regression was applied to the $S_{w,avg}$ versus Pc data.

$$S_{wavg} = cP_c^{\ b} \qquad (4)$$

The derivative of the fitted power-law equation can then be obtained, i.e.

$$\frac{dS_{wavg}}{dP_c} = bc\, P_c^{b-1} \qquad (5)$$

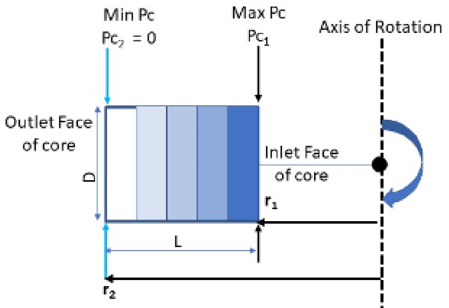

Fig. 2. Schematic of primary drainage capillary pressure measurement by using a centrifuge at ambient stress

2.5 Porous Plate Pc Tests at Reservoir Stress

Using the same samples from the centrifuge tests, Pc curves were measured via the porous plate (PP) method under high stress conditions. The samples were initially saturated with the prepared brine, before being loaded into a pressure cell at a confining pressure of 3,000 psi. Water-wet porous plates were used, allowing only the wetting phase (brine) to pass through. Pressurized Soltrol-130 was then introduced to displace the brine through the porous plate. The displaced brine volume was recorded and monitored at each capillary pressure step to determine the saturation equilibrium. Figure 3 shows a schematic of the experimental porous plate system.

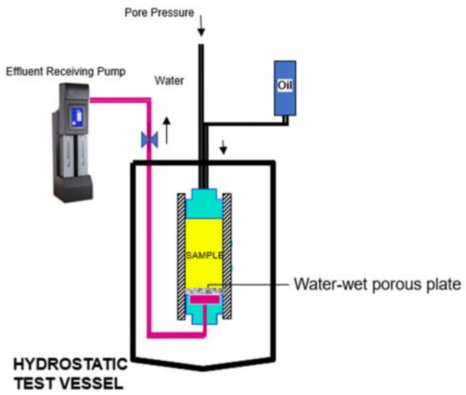

Fig. 3. The porous plate system for capillary pressure measurement at reservoir stress.

The PP test is a significantly slower process than centrifugation, each desaturation step required about 1-3 weeks to reach equilibrium, in terms of the brine production. The produced brine volume and the applied capillary pressure are then used to construct the Pc curve for the sample.

3 Results and Discussion

3.1 Centrifuge Pc Tests at Ambient Stress

In conducting centrifuge Pc tests, the samples were centrifuged at nine pressure steps controlled by RPM. At each RPM, the test took a minimum of 9 hrs to reach equilibrium fluid distribution. Figure 4 shows the generated curves with Pc calculated using Eq 2 and Sw using Eq 3 (Table 2). The trends of the Pc curves are typical, i.e., higher permeability samples generally show lower final water saturation at the highest RPM; which may be referred to initial water saturation, Swi, for the purpose of discussions (Fig. 5), although the word of irreducible may be debatable [26-27].

As illustrated in Figs. 4 and 5, the dolomite samples reached a much lower Swi compared to sandstone samples, while the limestone samples exhibited the highest across all permeability ranges (high, intermediate, and low). These results suggest probably that the dolomite samples have more uniform or interconnected pore-throats networks compared to sandstone and limestone samples.

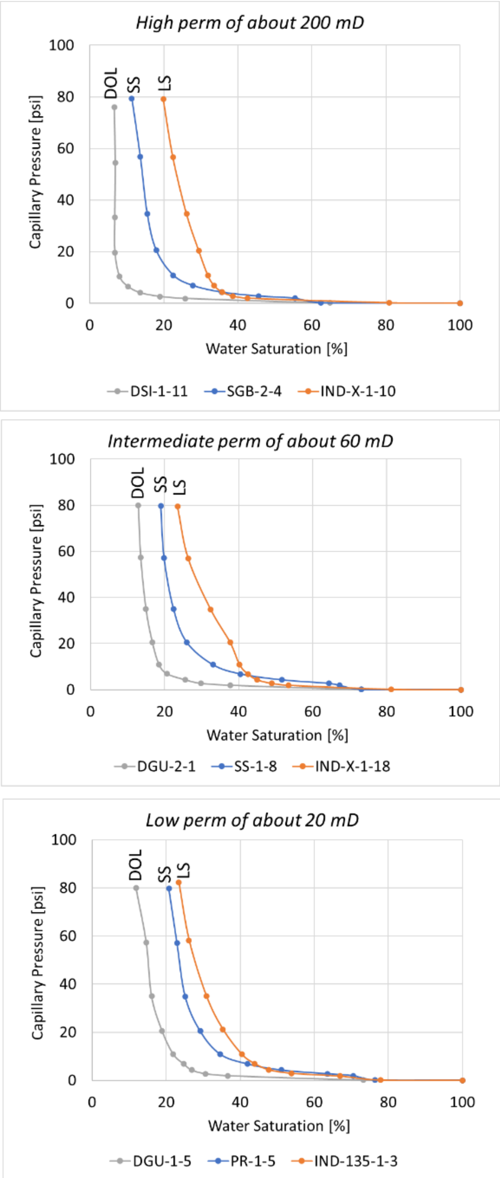

Fig. 4. Ambient centrifuge drainage capillary pressure curves of Set 1 (high perm), Set 2 (intermediate perm) and Set 3 (low perm) samples of lithology dolostone, sandstone, and limestone.

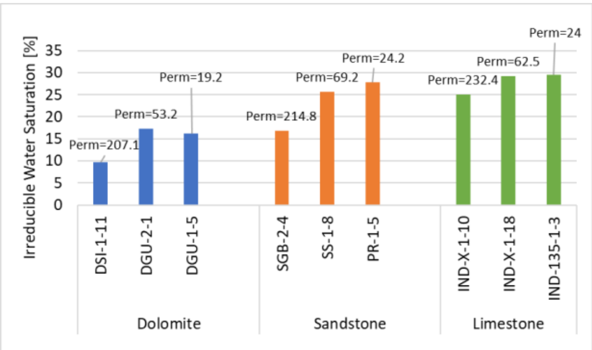

Fig. 5. Swi increases with decreaseF in permeability for each rock type of dolostone, sandstone, and limestone.

Table 2. Results of centrifuge capillary pressure measurements.

Set 1: High perm dolostone, sandstone, and limestone samples					
DSI-1-11		**SGB-2-4**		**IND-X-1-10**	
Pc, psi	Sw, %	Pc, psi	Sw, %	Pc, psi	Sw, %
0.0	100.0	0.0	100.0	0.0	100.0
0.1	64.9	0.1	62.4	0.1	80.9
1.8	25.8	1.9	55.4	1.9	42.7
2.6	19.0	2.7	45.7	2.7	38.6
4.1	13.6	4.2	35.6	4.2	35.8
6.5	10.3	6.8	27.9	6.8	33.6
10.4	8.1	10.8	22.6	10.8	31.9
19.6	6.8	20.5	18.0	20.4	29.4
33.3	6.8	34.7	15.5	34.6	26.1
54.5	6.9	56.8	13.6	56.6	22.5
76.1	6.7	79.4	11.4	79.1	19.9
Set 2: Intermediate perm dolostone, sandstone, and limestone samples					
DGU-2-1		**SS-1-8**		**IND-X-1-18**	
Pc, psi	Sw, %	Pc, psi	Sw, %	Pc, psi	Sw, %
0.0	100.0	0.0	100.0	0.0	100.0
0.1	73.1	0.1	73.2	0.1	81.2
1.9	37.8	1.9	67.2	1.9	53.5
2.7	29.8	2.7	64.4	2.7	48.9
4.3	25.6	4.3	51.7	4.2	45.1
6.8	20.7	6.8	40.5	6.8	42.5
10.9	18.5	10.9	33.0	10.9	40.3
20.6	16.7	20.6	26.0	20.5	37.7
35.0	15.0	34.9	22.5	34.8	32.5
57.3	13.6	57.1	19.9	57.0	26.4
80.0	12.9	79.8	19.0	79.6	23.5
Set 3: Low perm dolostone, sandstone, and limestone samples					
DGU-1-5		**PR-1-5**		**IND-135-1-3**	
Pc, psi	Sw, %	Pc, psi	Sw, %	Pc, psi	Sw, %
0.0	100.0	0.0	100.0	0.0	100.0
0.1	73.2	0.1	76.5	0.1	78.0
1.9	36.7	1.9	70.6	1.7	67.0
2.7	30.6	2.7	63.6	2.9	53.8
4.3	26.9	4.3	51.2	4.4	47.7
6.8	24.7	6.8	41.9	6.9	43.9
10.9	21.9	10.9	34.6	10.8	40.4
20.6	18.9	20.6	29.2	21.2	35.3
35.0	16.1	34.9	25.2	35.1	30.8
57.3	14.7	57.1	23.0	58.2	26.2
80.0	11.9	79.8	20.8	82.4	23.4

3.2 Porous Plate Pc Tests at Reservoir Stress

After the centrifugation tests, the samples were cleaned, dried and their properties were re-measured (Table 3), at both 500 psi and a applied reservoir confining pressure of 3,000 psi. The re-measured properties at 500 psi show comparable to those of the initial measurements (Table 1), indicating that the centrifuge tests did not measurably alter the samples' physical integrity of their original state.

Table 3. Rock properties after centrifuge Pc tests

Sample	Φ [%] 500psi	Φ [%] 3000psi	K [mD] 500psi	K [mD] 3000psi
DSI-1-11	14.57	14.36	199.97	198.73
DGU-2-1	11.57	11.45	55.13	54.84
DGU1-5	10.14	10.11	18.92	18.38
SGB-2-4	19.79	19.53	208.72	187.10
SS-1-8	20.95	20.75	68.27	66.01
PR1-5	17.37	17.31	22.74	22.01
IND-X-1-10	18.19	17.90	242.06	238.43
IND-X-1-18	18.04	17.75	63.01	60.77
IND-135-1-3	16.31	16.21	23.94	22.60

The nine samples were then saturated with the brine and loaded in HPHT (high pressure high temperature) cells to perform the PP tests, at 25°C. Once the applied confining pressure of 3,000 psi is stabilized, Soltrol-130 oil was introduced to the samples under various pre-set pressures, i.e., Pc. For each Pc, the volume of produced brine was recorded. Using the produced brine volume and the applied pressure, the PP Pc curves was obtained (Fig. 6 and Table 4).

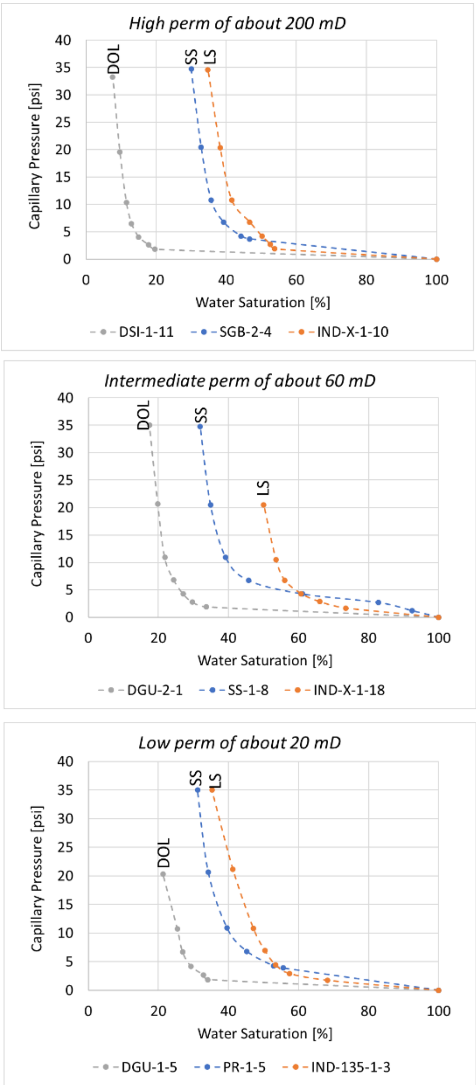

Fig. 6. Reservoir stress (3000 psi) porous plate drainage capillary pressure curves of Set 1 (high perm), Set 2 (intermediate perm) and Set 3 (low perm) samples of lithology dolostone, sandstone, and limestone.

Table 4. Porous plate capillary pressure vs water saturation.

Set 1: High perm dolostone, sandstone, and limestone samples					
DSI-1-11		SGB-2-4		IND-X-1-10	
Pc, psi	Sw, %	Pc, psi	Sw, %	Pc, psi	Sw, %
0.0	100.0	0.0	100.0	0.0	100.0
1.8	19.7	3.7	46.6	1.9	53.8
2.6	17.9	4.2	44.2	2.7	52.6
4.1	15.0	6.8	39.3	4.2	50.2
6.5	13.0	10.8	35.7	6.8	46.7
10.4	11.5	20.5	32.9	10.8	41.6
19.6	9.6	34.7	30.0	20.4	38.3
33.3	7.6			34.6	34.8
Set 2: Intermediate perm dolostone, sandstone, and limestone samples					
DGU-2-1		SS-1-8		IND-X-1-18	
Pc, psi	Sw, %	Pc, psi	Sw, %	Pc, psi	Sw, %
0.0	100.0	0.0	100.0	0.0	100.0
1.9	33.6	1.2	92.4	1.7	73.5
2.7	29.7	2.7	82.8	2.8	66.1
4.3	27.1	4.2	61.1	4.3	60.8
6.8	24.4	6.7	45.7	6.7	56.1
10.9	21.8	10.9	39.2	10.5	53.5
20.6	19.9	20.5	34.9	20.5	50.0
35.0	17.5	34.8	32.0		
Set 3: Low perm dolostone, sandstone, and limestone samples					
DGU-1-5		PR-1-5		IND-135-1-3	
Pc, psi	Sw, %	Pc, psi	Sw, %	Pc, psi	Sw, %
0.0	100.0	0.0	100.0	0.0	100.0
1.9	34.1	3.9	55.7	1.7	68.3
2.7	32.9	4.3	52.9	2.9	57.4
4.2	29.3	6.8	45.2	4.4	53.4
6.7	26.9	10.9	39.6	6.9	50.4
10.8	25.4	20.6	34.3	10.8	47.1
20.3	21.3	35.0	31.2	21.2	41.3
				35.1	35.3

3.2 Pc Comparison: porous plate vs. centrifuge

Figs. 7, 8 and 9 compare the ambient stress centrifuge drainage Pc curves (solid lines) with that of the reservoir stress PP Pc curves (dashed lines), for the high permeability Set 1, intermediate permeability Set 2, and low permeability Set 3 samples. The divergence between these curves is attributed to the effect of confining stress, and can be summarized as.

- Generally, the Pc curves shift to the higher Sw direction upon the application of stress, meaning that increased confining pressure leads to higher water retention across the Pc curve.

The magnitude of the stress effect varied significantly among the three rock types. Larger effects were observed for the sandstone and limestone samples compared to the dolostone, irrespective of their permeability. This variation is likely due to distinct mechanical properties of each rock type; stiffer rocks such as dolostone [28] in this study show more resistance to confining stress than more "softer" lithologies. Consequently:

- The magnitude of the effect of stress on Pc curves could be governed by the geomechanical characteristics in addition to the petrophysical properties. For further discussion of these observations we refer to [12, 13].

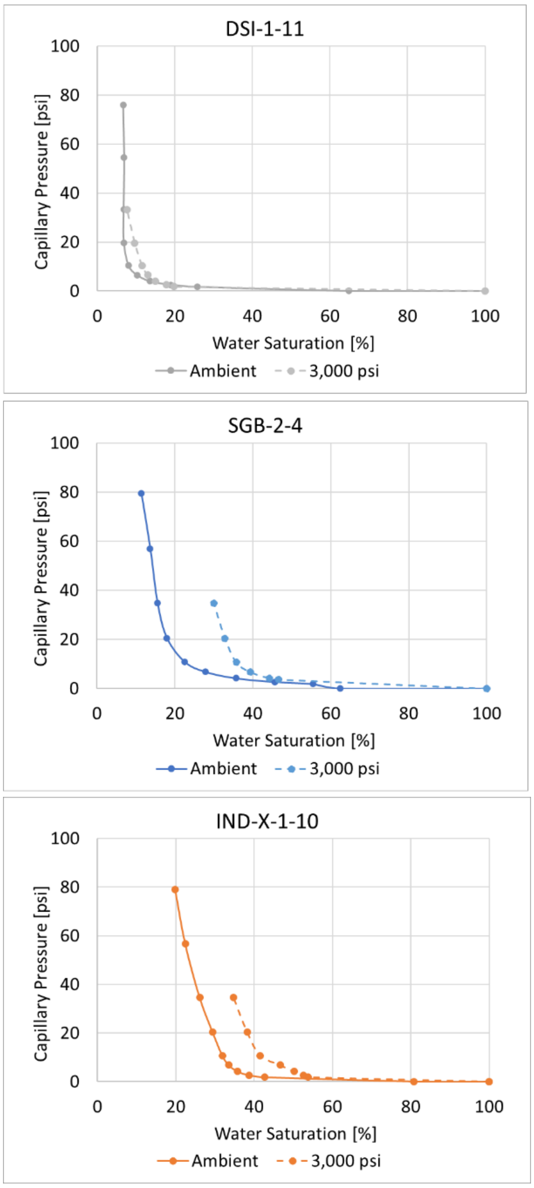

Fig. 7. Drainage Pc curves at reservoir stress of 3000 psi (dash) vs that at ambient (solid) for the high permeability Set 1 samples.

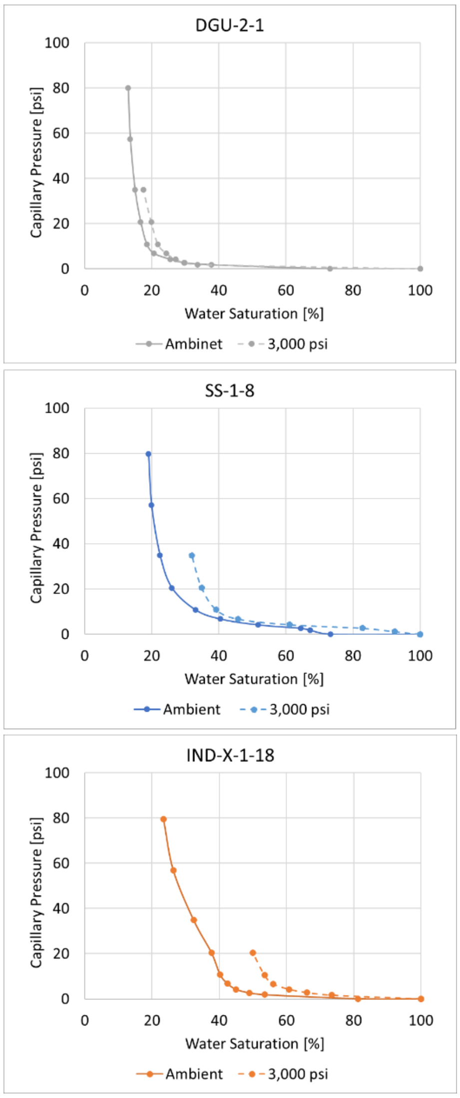

Fig. 8. Drainage Pc curves at reservoir stress of 3000 psi (dash) vs that at ambient (solid) for the intermediate permeability Set 2 samples.

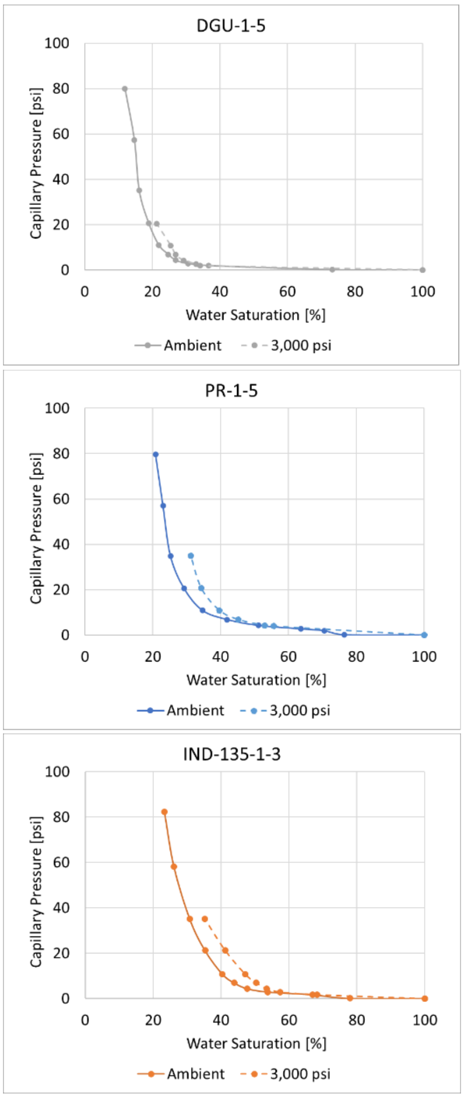

Fig. 9. Drainage Pc curves at reservoir stress of 3000 psi (dash) vs that at ambient (solid) for the low permeability Set 3 samples.

3.2.1 Effect of Stress on Pc- Beta Model

To convert the ambient stress centrifuge Pc curves to the reservoir stressed PP Pc curves, we initially utilized the model established by Al-Hamad et al. [13], which was developed for Indiana limestone samples. For this discussion, the established model is hereafter referred to as the Beta model.

The empirical Beta model is written as

$$S_w = aP_{cf} + b \tag{6}$$

Where

$$a = 0.04P_C^{-y} \tag{7}$$
$$b = xP_C^{-y} \tag{8}$$
$$x = 61.301 \tag{9}$$
$$y = 0.2 \tag{10}$$

Applying Eqs 6-10 to the limestone samples, the Pc curves at 3,000 psi were validated at ambient stress condition (Figure 10). The Beta model demonstrated high accuracy for two of the three samples; however, a noticeable discrepancy was observed for sample IND-X-1-10 between the corrected and measured ambient data. Thin-section analysis (Fig. 1) confirms consistent pore network characteristics or similarities [29] across the three limestone samples, suggesting that this deviation is likely attributed to the limitation and the universality of the Beta model rather than rock pore structure variations.

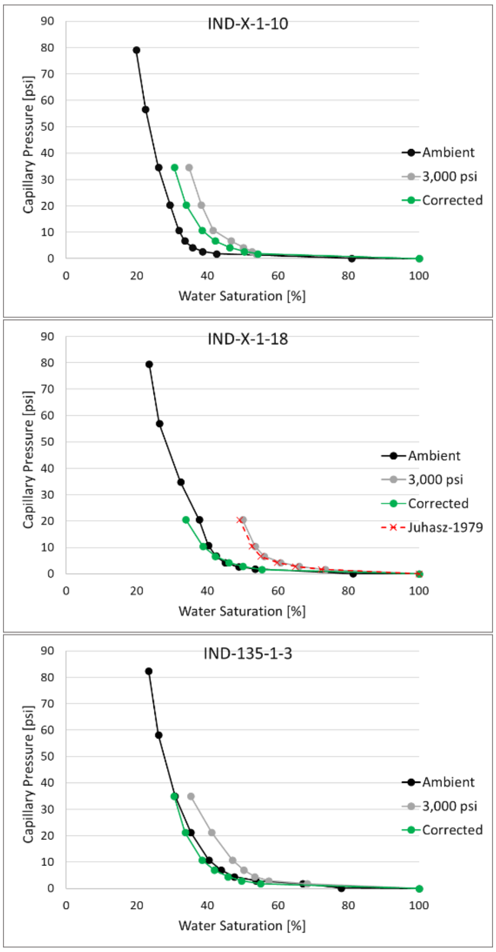

Fig. 10. Stress-corrected Pc curves in comparison with the centrifuge data for the limestone samples

Figure 11 compares the corrected and experimental capillary pressure data for the sandstone samples. The results indicate that, for this specific lithology, the Beta model fails to properly correct the Pc curves under elevated stress conditions. Given that these correlations were originally derived from high-resolution micro-CT data and digital rock simulations of limestone samples, these discrepancies suggest that the Beta model lacks universality across diverse rock types and mineralogy.

Additionally, the stress-adjustment method proposed by Juhasz [30] which utilizes porosity-stress correction was evaluated. When applied to carbonate sample IND-X-1-18 (Fig. 10) and sandstone sample SS-1-8 (Fig. 11), the model failed to accurately account for the impact of stress. These results suggest that:

- A simple porosity-dependent approach, such as Juhasz model, is insufficient for converting ambient Pc curves to reservoir-stressed conditions.

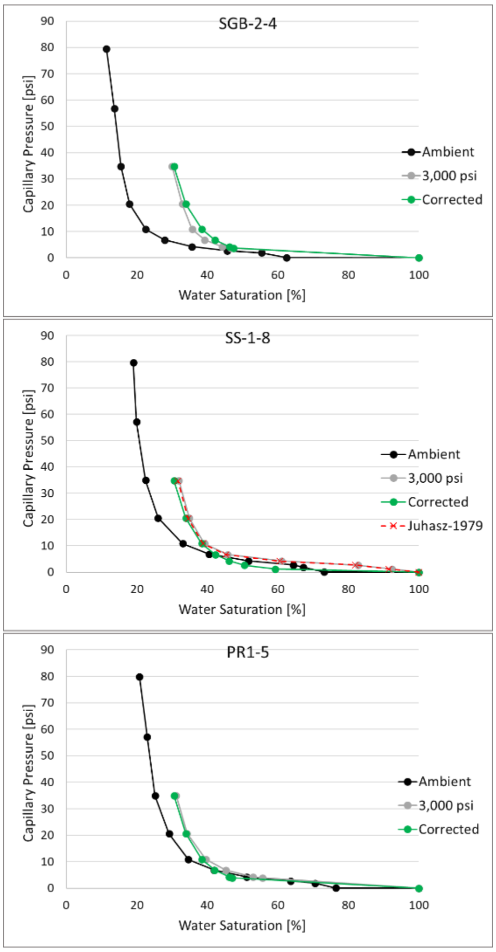

Fig. 11. Stress-corrected capillary pressure data in comparison with the centrifuge data for the sandstone samples

3.2.2 Effect of Stress on Pc- A General Model

Analysis of the centrifuge Pc data from this current study, in comparison with the previous study [13] indicates that the parameters x and y in Eqs. 9 and 10 must be treated as variables rather than constants to achieve a more robust stress correction. Further evaluation of the sandstone samples (Fig. 12) reveals that these variables are dependent on the water desaturation profiles, which is a function of rock mechanical stiffness (m). Each sample showed to exhibit a unique value for the slope (y) and intercept (x).

$$x = f_x(Sw, Pc, m) \quad (11)$$

$$y = f_y(Sw, Pc, m) \quad (12)$$

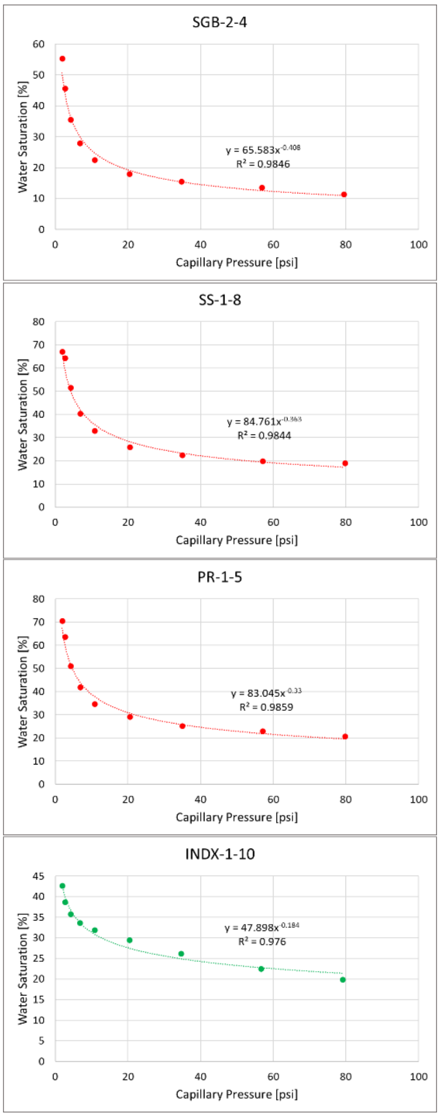

Fig. 12. Water saturation versus capillary pressure for the sandstone samples and high permeability limestone sample

By applying Eqs 11 and 12, the conversion between ambient and stress Pc curves was successfully achieved (Table 5, and Figs. 13). Furthermore, this generalized model (Eqs 11 and 12) effectively corrected the previously mismatched limestone sample (Fig. 10), as demonstrated in Fig. 14.

Table 5. Converted Sw from 3,000 psi to ambient stress for the selected samples using Eqs 6, 7, 8, 11 and 12

SGB-2-4					
Pc [psi]	**f**	**x**	**a**	**b**	**Sw_Corrected [%]**
0.00			0.0000	0.00	100
3.70			0.0023	38.46	38.49
4.23			0.0022	36.41	36.44
6.78	0.408	65.583	0.0018	30.04	30.06
10.82			0.0015	24.82	24.84
20.46			0.0012	19.14	19.16
34.74			0.0009	15.42	15.44
SS-1-8					
Pc [psi]	**f**	**x**	**a**	**b**	**Sw_Corrected [%]**
0	0.363	84.761	0	0	100
1.19			0.0038	79.57	79.63

2.68			0.0028	59.26	59.30
4.24			0.0024	50.17	50.21
6.70			0.0020	42.49	42.52
10.90			0.0017	35.61	35.64
20.49			0.0013	28.32	28.34
34.77			0.0011	23.37	23.39
PR1-5					
Pc [psi]	f	x	a	b	Sw_Corrected [%]
0	0.330	83.045	0	0	100
3.89			0.0026	53.04	53.08
4.26			0.0025	51.48	51.51
6.83			0.0021	44.05	44.08
10.90			0.0018	37.75	37.78
20.62			0.0015	30.59	30.61
35.01			0.0012	25.69	25.71
INDX-1-10					
Pc [psi]	f	x	a	b	Sw_Corrected [%]
0	0.184	47.895	0	0	100
1.87			0.0036	42.68	42.74
2.70			0.0033	39.90	39.94
4.21			0.0031	36.76	36.81
6.76			0.0028	33.70	33.74
10.78			0.0026	30.92	30.96
20.39			0.0023	27.50	27.54
34.62			0.0021	24.95	24.98

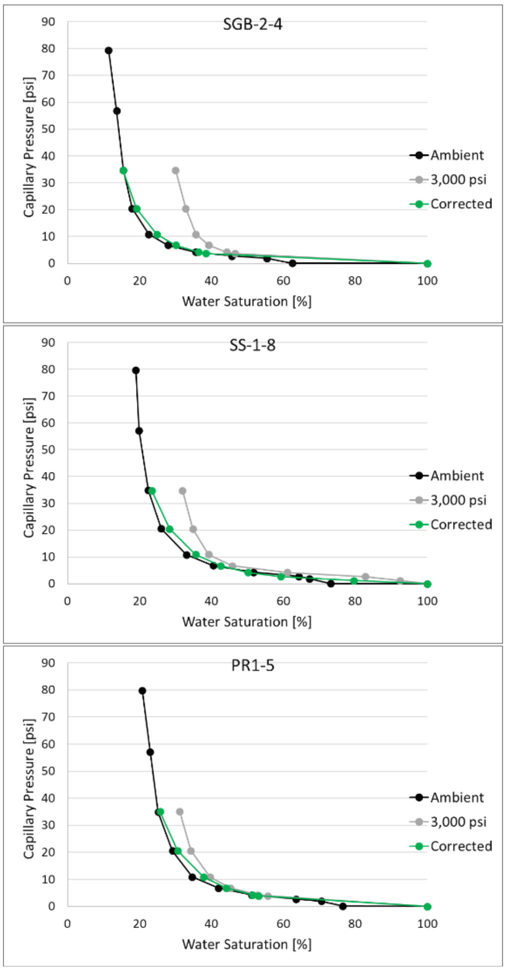

Fig. 13. Stress-corrected vs measured ambient Pc curves for the sandstone samples

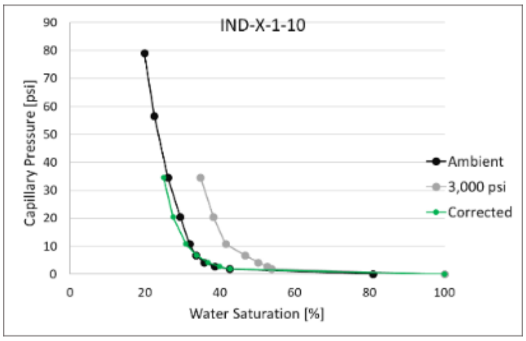

Fig. 14. Stress-corrected vs measured ambient Pc curves for IND-X-1-10.

4 Conclusions

This study builds upon our previous study [13], leading to the following conclusions:

- Increased confining stress consistently shifts Pc curves towards higher water saturation direction, indicating that water retention increases as a function of applied stress.
- A generalized Pc stress-correction model (Eqs 6, 7, 8, 11, and 12) was developed and validated using ambient centrifuge Pc and 3,000 psi stressed porous plate Pc curves. The model proved robust across dolostone, limestone, and sandstone samples with permeabilities of 20 mD to 250 mD and porosities of 10% to 20%.
- The impact of stress on Pc curves is primarily governed by rock stiffness, rock mechanical properties andthe petrophysical characteristics (e.g., permeability or porosity).

5 Acknowledgments

The authors would like to thank Vijaya Puvvala for his valuable contributions to this study.

6 Nomenclature

C	constant
h	height above free water level
m	rock mechanical properties; stiffness
P	pressure
r	distance from the centrifuge center to the core face
R	pore throat radius
S	saturation
x	model fitting parameter
ρ	fluid density
σ	water-oil interfacial tension
θ	water-oil-rock contact angle
Φ	porosity
K	permeability

Subscripts

1, 2	inlet and outlet faces of centrifuge core samples
avg	average
C	capillary
cf	confining pressure/stress
o	oil

t pore throat
w water

Superscript
y model parameter

7 References

1. J.W. Amyx, D.M. Bass, and R.L. Whiting. Petroleum Reservoir Engineering – Physical Properties, McGraw-Hill Book Company (1960)
2. H.W. Brown. Capillary Pressure Investigations, SPE Petroleum Branch Fall Meeting, Oklahoma City, 3–5 Oct (1951)
3. B. Harrison and X.D. Jing. Saturation Height Methods and Their Impact on Volumetric Hydrocarbon in Place Estimates, SPE-71326, SPE ATCE, New Orleans, 30 Sept–3 Oct (2001)
4. S.K. Masalmeh and X.D. Jing. Capillary Pressure Characterization of Carbonate Reservoirs: Relationship between Drainage and Imbibition Curves, SCA2006-16, Int'l Symp of the Society of Core Analysts, Trondheim, 12–16 Sept (2006)
5. L. Lang, L. Venkataramanan, S. Wang, F.C. Canesin, V.-M. Gkortsas, K. Cig, and T.M. Habashy. Estimating In-Situ Relative Permeability and Capillary Pressure From Multiphysics Wireline Measurements, SPWLA 59th Annual Logging Symp, Old Windsor, 2–6 June (2018)
6. J. Ma, L. Liang, M. van Steene, & S. Ma. Pore system characterization of carbonate formations: a Multiphysics approach through acoustic & NMR measurements, SPWLA-2023-0051, SPWLA 64th Annual Symp, 10-14 June, Conroe (2023)
7. J. Ma, L. Liang, M. Al-Hamad, M. van Steene, S. Ma, and W. Abdalla. Aspect ratio dependent pore size distribution from MICP measurement, IPTC-23659, IPTC, 12-14 Feb, Dhahran, Saudi Arabia. (2024)
8. J. Ma, L. Liang, M. Al-Hamad, M. Van Steene, O. Sindt, S. Ma, J. Luo, and Y Hu. Enhanced characterization of pore size distribution from NMR T2 by integrating pore shape aspect ratio and sonic measurements, paper SPWLA-2025-0074, SPWLA 66th ALS, 17-21 May, Dubai, UAE. (2025)
9. S. Ma, A. Al-Hajari, D. Kersey, et al. Enhanced petrophysics: integration of core & log data for improved reservoir saturation monitoring, SPE-106350, SPEKSA Tech Symp. (2006)
10. M. Suhrer, J. Toelke, X. Nie, & S. Ma. Upscaling method for obtaining primary capillary pressure and resistivity index with digital rock physics, IPTC-20035, IPTC, Saudi Arabia, 13-15 Jan. (2020)
11. D. Koroteev, O. Dinariev, N. Evseev, D. Klemin, A. Nadeev, S. Safonov, O. Gurpinar, S. Berg, C. van Kruijsdijk, R. Armstrong, M.T. Myers, L. Hathon, and H. de Jong. Direct Hydrodynamic Simulation of Multiphase Flow in Porous Rock, Petrophysics, 55(3), 294-303 (2014)
12. M. Al Hamad, D. Klemin, S. Ma, and W. Abdallah. Digitally Derived Capillary Pressure Data for Reservoir Evaluation, SPE MEOS and GEO, Manama, 19–21 Feb (2023)
13. M. Al-Hamad, D. Klemin, S. Ma, and W. Abdallah. Insights of Core Analysis Data Interpretation by Use of Digital Rock Physics, SPWLA 65th Annual Logging Symp, Rio de Janeiro, 19-22 May (2024)
14. S.A. Bertels, A.R. DiCarlo, and M.J. Blunt. Measurement of aperture distribution, capillary pressure, relative permeability, and in situ saturation in a rock fracture using CT scanning, Water Resources Research, 37(3), 649–662 (2001)
15. Z.S. Omoregie. Factors Affecting the Equivalency of Different Capillary Pressure Measurement Techniques, SPE ATCE, New Orleans, 5–8 Oct (1986)
16. N.R. Morrow. Wettability and Its Effect on Oil Recovery, Journal of Petroleum Technology, 42(12), 1476–1484 (1990)
17. D. Huo and S.M. Benson. Experimental investigation of CO2-liquid capillary pressure in reservoir rocks at reservoir conditions, Advances in Water Resources, 92, 135–150 (2016)
18. P. Lian and L. Cheng. The characteristics of relative permeability curves in naturally fractured carbonate reservoirs, J. Canadian Petroleum Technology, 51(02), 137–142 (2012)
19. Y. Watanabe, C.H. Christensen, J.O. Helland, and K. Mogensen. Historical perspective on the capillary pressure function in porous media based on relative permeabilities of two immiscible fluids: Application of capillary bundle models and validation using experimental data, Advances in Colloid and Interface Science, 226, 42–63 (2015)
20. N. Morrow, K. Brower, S. Ma, & J. Buckley. Fluid flow in healed tectonic fractures, *JPT*, pp.1310, Oct. (1990)
21. S.A. Holditch. Tight Gas Sands, Journal of Petroleum Technology, 58(06), 86–93 (2006)
22. A. AlZoukani, G. Aidagulov, F. Ali, M. Al-Hamad, and W. Abdallah. Robust Centrifuge Data Processing for Tight and Permeable Rock Samples, IPTC, Riyadh, 21–23 Feb (2022)
23. R.M. Cluff, S.G. Cluff, and C.M. Murphy. The use of capillary pressure data to calibrate log-derived water saturation in tight gas sands, Paper SPE-124317-MS, presented at the SPE ATCE, New Orleans, 4–7 Oct (2009)
24. S. Ma, M. Jiang, and N. Morrow. Correlation of capillary pressure relationships and calculations of permeability, SPE-22685, the 66th SPE ATCE, Dallas, Oct. 6-9 (1991)

25. A. AlZoukani, G. Aidagulov, F. Ali, M. Al-Hamad, and W. Abdallah. Robust Centrifuge Data Processing for Tight and Permeable Rock Samples, IPTC, Riyadh, 21–23 Feb (2022)

26. S. Ma and N. Musharfi: Composition and methods to recover irreducible water for enhanced formation evaluation, US Patent 10,633,574, 28 April (2020).

27. H. Qatari, S. Ma, T. Okashah, and N. Alsaleh. Method to recover connate water from reservoir cores using centrifuge and surfactant-enhanced oil for formation evaluation, paper SCA 2026-020, SCA 2026 Annual Symp, Aug 17-21, Mexico City, Mexico, (2026)

28. D. Cantrell, P. Swart, R. Handford, et al.,. Geology and production significance of dolomite. GeoArabia, v.6, no.1, pp.45-59 (2001)

29. S. Ma & N. Morrow. Similarity of pore structure and the selection of core samples for tests of scaling, Proc. 9th Wyoming EOR Symposium, May 12-13, Casper, Wyoming. (1993)

30. I. Juhasz. The central role of formation water salinity in the evaluation of shaly formations, SPWLA 20th Annual Logging Symp, Paper AA, 1–32 (1979)